nature genetics

The imprinted gene *Magel2* regulates normal circadian output

Serguei V Kozlov[1], James W Bogenpohl[2], Maureen P Howell[3], Rachel Wevrick[4], Satchin Panda[5], John B Hogenesch[6], Louis J Muglia[3,7], Russell N Van Gelder[8], Erik D Herzog[2] & Colin L Stewart[1,9]

Mammalian circadian rhythms of activity are generated within the suprachiasmatic nucleus (SCN). Transcripts from the imprinted, paternally expressed *Magel2* gene, which maps to the chromosomal region associated with Prader-Willi Syndrome (PWS), are highly enriched in the SCN. The *Magel2* message is circadianly expressed and peaks during the subjective day. Mice deficient in *Magel2* expression entrain to light cycles and express normal running-wheel rhythms, but with markedly reduced amplitude of activity and increased daytime activity. These changes are associated with reductions in food intake and male fertility. Orexin levels and orexin-positive neurons in the lateral hypothalamus are substantially reduced, suggesting that some of the consequences of *Magel2* loss are mediated through changes in orexin signaling. The robust rhythmicity of *Magel2* expression in the SCN and the altered behavioral rhythmicity of null mice reveal *Magel2* to be a clock-controlled circadian output gene whose disruption results in some of the phenotypes characteristic of PWS.

PWS is caused by the loss of paternal expression of a cluster of genes at human chromosome 15q11-q13. It is a genetic obesity syndrome characterized by hyperphagia, sleep apnea, hypogonadism and growth hormone deficiency, suggesting abnormalities in hypothalamic function[1].

Within the PWS region, four genes—small nuclear ribonucleoprotein N (*SNURF-SNRPN*), makorin-3 (*MKRN3*, also called *ZNF127* or *ZFP127*), necdin (*NDN*) and mage-like-2 (*MAGEL2*)—encode proteins with paternal allele–specific expression. In addition to these translated genes, other nontranslated transcripts are paternally expressed[2]. Mice deficient in *Snurf-Snrpn* and *Mkrn3* show no overt effects (refs. 3,4 and C.L.S. and A.H. Carey, unpublished observations), whereas deletion of the region upstream of *Snurf-Snrpn* (the imprinting center, or IC) results in aberrant expression of the genes and early postnatal lethality[3,4]. Mice inheriting a deletion of *Ndn* from their fathers develop perinatal, strain-dependent, fatal respiratory distress, owing to defects in the central respiratory rhythm-generating center[5–7]. These phenotypes as well as other changes, including increased skin-scraping activity, improved spatial learning and structural abnormalities of the hypothalamus, are consistent with some of the pathologies observed in PWS[8,9]. These observations indicate that PWS results from contiguous defects in gene expression, with loss of function of individual genes contributing to specific phenotypes that, when combined, comprise PWS[1].

The remaining structural gene in the PWS region, *MAGEL2*, is an intronless gene of unknown function with homology to *NDN*[10,11]. In the mouse embryo, *Magel2* is expressed in the hypothalamus, cerebral cortex and spinal cord[12], but little is known about its spatial and temporal expression in adults except that *Magel2* transcripts are highly enriched and rhythmically expressed in the SCN[13]. To assess the potential role of *Magel2* in circadian timekeeping and the effect loss of its paternal expression has on mice and the development of PWS, we examined its expression in the adult mouse brain and determined the effects of *Magel2* deletion on activity rhythms.

We used a *lacZ* knock-in allele (**Supplementary Fig. 1a** online) to define *Magel2* expression during embryogenesis and in the adult brain. Around mid-gestation, *Magel2* transcription was restricted to the central nervous system (CNS)—in particular, the neural tube, forebrain, midbrain and embryonic hypothalamus. Expression in the peripheral nervous system was detected in the dorsal root ganglia and peripheral neurons innervating limb and trunk muscles (**Fig. 1a**,**b**). In non-neuronal tissues, *Magel2* expression was confined to the genital tubercle, midgut region and placenta (**Fig. 1b** and **Supplementary Fig. 2c** online). Embryonic *Magel2* expression therefore differed from the expression of its closest homolog, *Ndn* (found in almost all postmitotic neurons[5,11]).

In the adult brain, the majority of *Magel2*-positive neurons reside in the hypothalamic region, with the exception of a few neurons in the external capsule adjacent to the cortex, the lateral and triangular septal

[1]Cancer and Developmental Biology Laboratory, National Cancer Institute, Frederick, Maryland 21702, USA. [2]Department of Biology, Washington University, St. Louis, Missouri 63130, USA. [3]Department of Pediatrics, Washington University School of Medicine, St. Louis, Missouri 63110, USA. [4]Department of Medical Genetics, University of Alberta, Edmonton, Alberta, Canada T6G 2H7. [5]Regulatory Biology Laboratory, Salk Institute for Biological Studies, La Jolla, California 92037, USA. [6]Genomics Institute of Novartis Research Foundation, La Jolla, California 92121, USA. [7]Departments of Molecular Biology and Pharmacology and [8]Department of Ophthalmology and Visual Sciences, Washington University School of Medicine, St. Louis, Missouri 63110, USA. [9]Present address: Institute for Medical Biology, #03-03 Proteos, 61 Biopolis Drive, Singapore 113867, Singapore. Correspondence should be addressed to C.L.S. (stewartc@ncifcrf.gov or colin.stewart@imb.a-star.edu.sg).

Received 28 March; accepted 17 July; published online 23 September 2007; doi:10.1038/ng2114

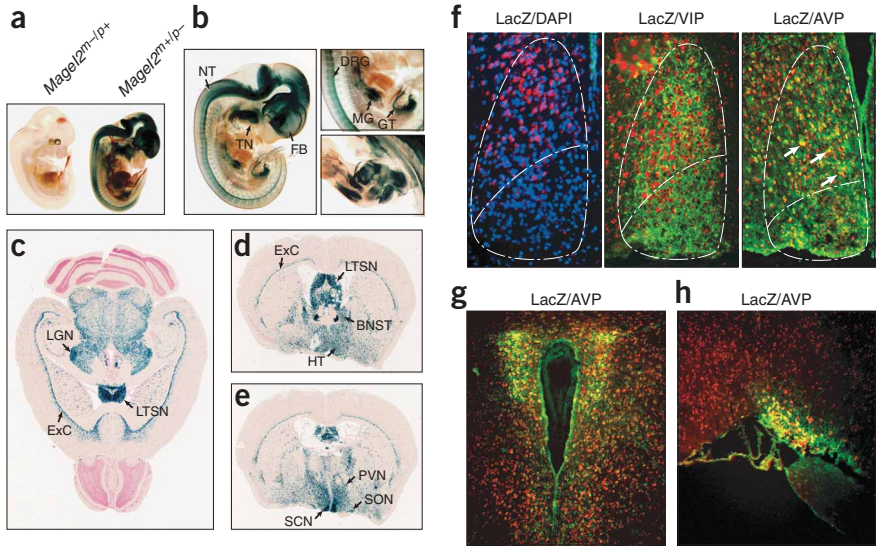

Figure 1 Expression patterns of the *Magel2* transcript, visualized using LacZ histochemistry, show both the paternal expression of *Magel2 in vivo* and the tissue specificity of *Magel2* expression in the embryonic and adult nervous systems. (**a**) *Magel2* expression depends on the parental transmission of *lacZ* allele. The paternally transmitted *lacZ* allele is fully functional, as indicated by intense blue staining (right embryo), whereas the maternally transmitted allele is completely silenced (left embryo). (**b**) *Magel2* embryonic expression in the developing nervous system, genital tubercle (GT), midgut (MG) region (top right photo) and peripheral nervous system innervating the hind-limb muscles (bottom right photo). DRG, dorsal root ganglia; FB, forebrain region; NT, neural tube; TN, tongue. (**c**–**e**) Expression of *Magel2* in the adult brain at a midlevel horizontal section (**c**), and coronal sections at the level of the anterior commissure (**d**) or the optic chiasma (**e**). BNST, bed nucleus of stria terminalis; ExC, external capsule; HT, hypothalamus; LGN, lateral genucleate nucleus; LTSN, lateral and triangular septal nuclei. (**f**) *Magel2* expression is specifically localized to a subset of dorsolateral SCN neurons. *Magel2*-expressing cells were labeled by LacZ-specific immunostaining (magenta) combined with staining of either nuclei (by DAPI, left), VIP (middle) or arginine-vasopressin (AVP, right). *Magel2* was expressed selectively in a subset of dorsolateral SCN neurons. *Magel2* also colocalized with vasopressin-immunoreactive neurons in the PVN (**g**) and the SON (**h**) (yellow fluorescence).

nuclei (**Fig. 1c**), and the bed nucleus of stria terminalis (**Fig. 1d**). The hypothalamic structures with the most prominent *Magel2* expression were the magnocellular system composed of the SCN and the paraventricular (PVN) and supraoptic (SON) nuclei (**Fig. 1e**). Other regions expressing *Magel2* were the lateral geniculate nuclei and the amygdala, although in both structures only a subset of neurons showed *Magel2* transcription (data not shown).

The SCN is comprised of two anatomically and molecularly distinct neuronal populations. Neurons located in the ventrolateral part of the SCN receive a daylight-modulated input from the retina via the retinohypothalamic tract[14]. The ventrolateral neurons express vasoactive intestinal peptide (VIP) and synapse onto the adjacent population of neurons located in the dorsomedial portion of the SCN. Dorsomedial neurons specifically express the neuropeptide vasopressin and relay signals to target structures for circadian output, including the nuclei of the subparaventricular zone, pineal gland and pituitary[15,16].

We localized *Magel2*-positive neurons in the SCN using double immunohistochemistry with staining for LacZ and either VIP or vasopressin. *Magel2-lacZ*–positive neurons were predominantly localized to the dorsal part of the SCN, whereas the DAPI-stained neurons in the ventral half were mostly *Magel2* negative (**Fig. 1f**). The LacZ-positive cells overlapped with those expressing vasopressin, whereas there was only minimal overlap in expression of LacZ and VIP markers, probably owing to the proximity of VIP-positive neural fibers traversing the dorsal area. An overlap of vasopressin-positive neurons with those expressing LacZ was also found in other components of the magnocellular system—specifically, in the PVN (**Fig. 1g**) and SON (**Fig. 1h**). These results reveal that the subset of SCN neurons expressing *Magel2* overlap with the population of SCN dorsal neurons that function as modulators and conductors of a major pacemaker circadian output pathway to target organs and tissues[16].

Magel2 expression, as detected by *in situ* measurement of the abundance of messenger RNA transcripts in the SCN and the arcuate (AN) and ventromedial (VMH) nuclei, was rhythmic in a light-dark cycle, peaking in the late day (**Fig. 2a**; SCN, 23.2 ± 2.5 relative optical density (OD) grayscale units at its peak expression; AN, 80.8 ± 17.9; VMH, 30.8 ± 2.6). The SCN showed a 3.7-fold change in expression between the peak and trough of the rhythm, the AN showed a 5.1-fold change between peak and trough, and the VMH showed a 10.3-fold change (**Fig. 2b**). Rhythmic expression of *Magel2* persisted in the SCN in constant darkness (**Fig. 2c**), with a 3.0-fold decrease from the middle of the subjective day (72.0 ± 14.4) to the beginning of the subjective night (23.8 ± 6.0). In addition to the SCN, AN and VMH, *Magel2* expression was apparent in the PVN in constant darkness, but not in light-dark conditions. Expression peaked in the AN, VMH and PVN during the subjective day (73.5 ± 7.3, 45.8 ± 1.3 and 44.5 ± 2.7 relative OD units, respectively) and reached a minimum in the beginning of the subjective night (44.7 ± 9.2, 14.4 ± 2.5 and 16.7 ± 3.2). The AN showed a 1.6-fold change, the VMH showed a 3.2-fold change, and the PVN showed a 2.7-fold change (**Table 1**).

To determine whether *Magel2* is essential for circadian cycles, we derived C57Bl6 mice deficient in *Magel2* expression by paternal inheritance of the *lacZ* knock-in allele (**Supplementary Fig. 1a**). A complete lack of β-galactosidase activity encoded by a maternally inherited allele was noted both in mid-gestation embryos (**Fig. 1a**) and in the adult brain (data not shown), indicating tight, cell-specific control of maternal *Magel2* transcriptional repression. These mice (*Magel2*$^{m+/p-}$), whose phenotypes were effectively null for *Magel2* expression, were weaned at a frequency approximately 10% lower than that expected, suggesting that loss of *Magel2* expression may have some detrimental effect on early postnatal viability (**Supplementary Table 1** online). However, the pups that survived did not show any major abnormalities in size or weight even by 2 years of age. There was no indication that loss of *Magel2* had a substantial effect on fetal development or placental growth, as *Magel2* was strongly expressed in the placenta (**Supplementary Fig. 2a–c**). Analysis of the expression of *Magel2* along with that of two neighboring imprinted genes, *Ndn* and *Mkrn3*, by semiquantitative reverse-transcription (RT)-PCR confirmed the absence of *Magel2* transcripts in brain samples but revealed slightly elevated levels of *Ndn* expression, whereas transcription of the *Mkrn3* gene was unaffected (**Supplementary Fig. 1c**).

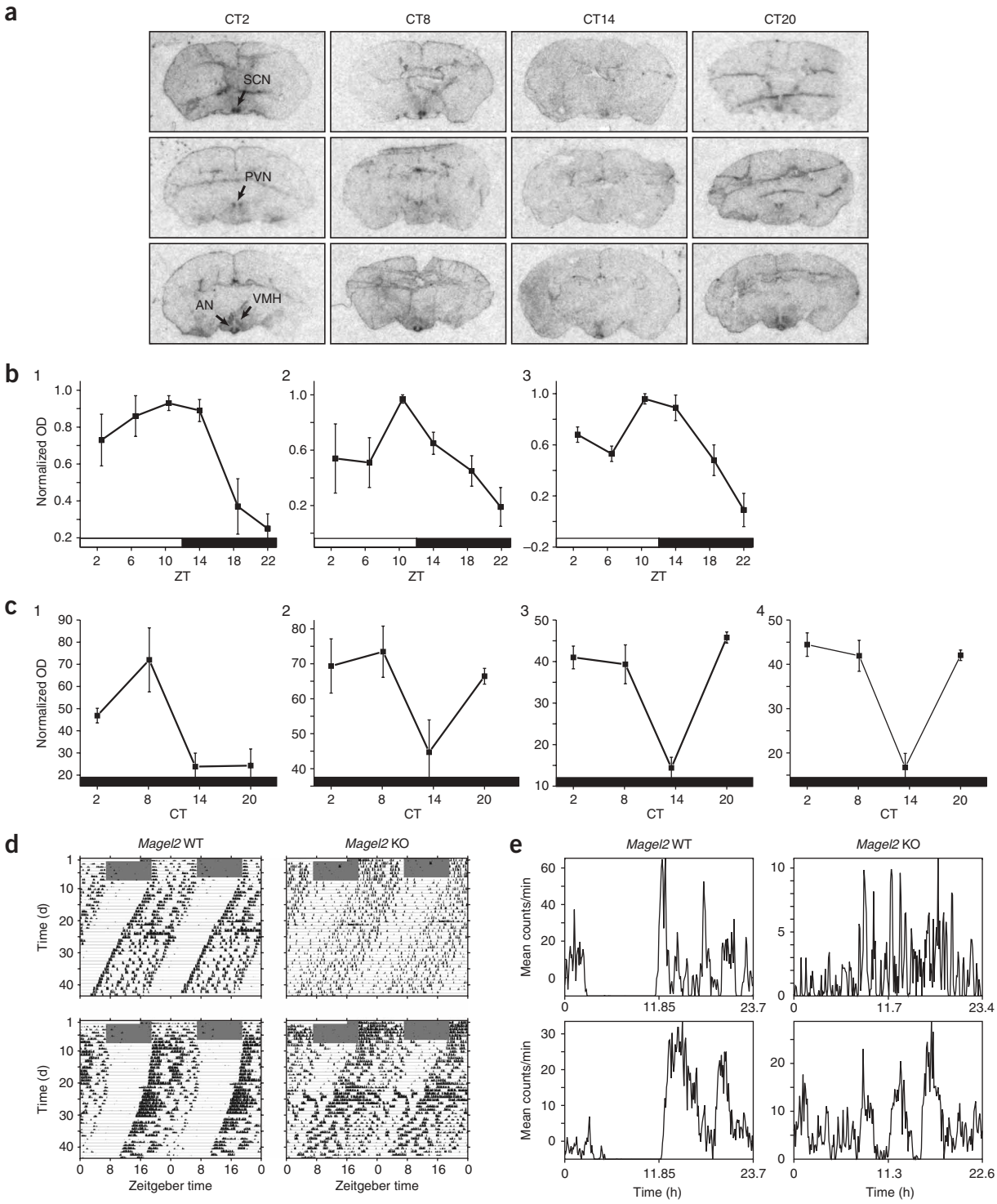

Figure 2 CNS *Magel2* transcript levels change during circadian cycles, and loss of *Magel2* expression affects activity cycles. (**a**) Representative results of *in situ* hybridization of *Magel2*, showing expression in the SCN, PVN, AN and VMH at four time points. Coronal brain sections were 20 μm thick and were taken from adult mice that were free-running in constant darkness. (**b**) *Magel2* mRNA expression in the SCN (1), AN (2) and VMH (3), as measured from brain sections taken from mice in a 12 h/12 h light/dark light cycle (lights were on from ZT0 to ZT12). Mean optical densities from three independent *in situ* hybridizations (three mice per time point) were normalized to the peak expression for each mouse. *Magel2* expression peaked before the light-to-dark transition in all three brain areas. Error bars represent s.e.m. (**c**) *Magel2* expression in the SCN (1), AN (2), VMH (3) and PVN (4) as measured by *in situ* hybridization of mouse brains taken from animals in constant darkness. OD (mean ± s.e.m., three mice per time point) reached a maximum in the late subjective day in all four areas. (**d**) Representative running-wheel actograms from two wild-type mice (left) and two *Magel2*$^{m+/p-}$ mice (right). All mice were entrained to 12 h/12 h light/dark for 1 week and then released into constant darkness. *Magel2*-null mice expressed circadian rhythms in locomotor activity, but of diminished amplitude, with more activity during the subjective day than their wild-type siblings. (**e**) Average daily activity profiles from days 26–35 in constant darkness of the same two wild-type mice (left) and two *Magel2*$^{m+/p-}$ mice (right). Note the fragmented night-time activity of the *Magel2*$^{m+/p-}$ mice.

Table 1 Changes in *Magel2* transcript levels in the SCN, AN, VMH and PVN brain nuclei

	Average peak OD in light-dark	Amplitude in light-dark	Average peak OD in constant darkness	Amplitude in constant darkness
SCN	23.2	3.7-fold	72.0	3.0-fold
AN	80.8	5.1-fold	73.5	1.6-fold
VMH	30.8	10.3-fold	45.8	3.2-fold
PVN	N/A	N/A	44.5	2.7-fold

Shown are the average absolute peak OD values and amplitudes of rhythms in expression (calculated as fold change by dividing the peak value by the trough value) for all four brain nuclei that showed *Magel2* staining in the *in situ* hybridization assay. The PVN did not reliably show expression of *Magel2* in light-dark in the *in situ* hybridization experiments. Average peak OD values cannot necessarily be compared between light-dark and constant-darkness conditions, because those experiments were performed with different radioactive probes with different specific activities.

Table 2 *Magel2*$^{m+/p-}$ mice have altered activity levels and durations

	Period by χ^2	χ^2 amplitude	Counts per day	Bouts per day	Bout length
Wild-type	23.75 h	764.7	12,770	4.9	83.1 min
Magel2$^{m+/p-}$	23.51 h	397.3	3,047	8.5	21.8 min
P-value	0.15	<0.001	0.0023	0.0026	<0.001

Average measurements of period, amplitude, counts per day, bouts per day and bout length of wild-type and *Magel2*$^{m+/p-}$ mice are summarized. Measurements were made over days 26–35 of constant darkness and are averaged over all wild-type ($n = 11$) and all *Magel2*$^{m+/p-}$ mice ($n = 9$).

We then tested the role of *Magel2* in circadian behavior by recording running-wheel activity of mice lacking the paternal *Magel2* allele. Wild-type ($n = 11$) and *Magel2*$^{m+/p-}$ ($n = 9$) mice entrained similarly during 1 week in a 12 h/12 h light/dark cycle and free-ran with similar periods during days 26–35 of constant darkness (23.75 ± 0.06 h, 23.51 ± 0.17 h; $P = 0.15$, Student's *t*-test). The *Magel2*$^{m+/p-}$ mice, however, ran significantly less than the wild-type controls: the average counts per day during days 26–35 of constant darkness were 3,047 ± 930 for *Magel2*$^{m+/p-}$ and 12,770 ± 2,343 for wild-type mice (**Table 1**; $P = 0.002$). *Magel2*$^{m+/p-}$ mice consistently ran in more frequent and shorter bouts than their wild-type siblings did (8.5 ± 0.7 and 4.9 ± 0.4 bouts per day, respectively; $P = 0.003$). *Magel2*$^{m+/p-}$ mice showed an average bout length of 21.8 ± 4.3 min, significantly shorter than that of wild-type mice (83.1 ± 15.4 min; **Table 1**; $P < 0.001$). The percentage of daily activity occurring during the subjective night was significantly lower in *Magel2*$^{m+/p-}$ mice (76.9 ± 2.8%) than in wild-type mice (86.6 ± 2.5%; $P = 0.006$), as shown by average daily activity profiles (**Fig. 2d**,**e**). Furthermore, rhythms of *Magel2*$^{m+/p-}$ mice had significantly lower χ^2 periodogram amplitudes than did those of wild-type mice (**Table 2**; 397.3 ± 14.3, 764.7 ± 67.9; $P < 0.001$).

Circadian expression in the liver of two pacemaker genes, *Clock* and *Per1*, was unaffected in *Magel2*$^{m+/p-}$ mice, indicating preservation of the underlying circadian pacemaker, despite loss of *Magel2* expression (**Supplementary Fig. 1d**). In addition, an array analysis of gene expression patterns in the magnocellular nuclei, at the time *Magel2* levels peaked, did not reveal any substantial change in the expression of genes that comprise the central clock mechanism (C.L.S., J.B.H. and S.P., unpublished observations). The function of the SCN is to coordinate phase relationships and rhythmicity of peripheral clocks[17]. This suggests the existence of specific genes that confer a unique circadian phenotype to the SCN pacemaker. One of these specific genes would seem to be *Magel2*.

One of the most noteworthy aspects of PWS is that after an initial postnatal period of hypotonia and difficulty in feeding, children develop hyperphagia and as a consequence become obese. Although *Magel2*$^{m+/p-}$ mice did not become overtly obese, we analyzed their feeding behavior and food intake. After starvation for 24 h, food intake (provided *ad libitum*) was monitored for a 48-h period in 6-week-old mice. The *Magel2*$^{m+/p-}$ mice showed slightly but significantly lower food intake ($P < 0.06$; $n = 8$; **Fig. 3a**,**b**). We also found that systemic levels of the hormone ghrelin, elevated levels of which are associated with increased appetite, were slightly lower in the *Magel2*$^{m+/p-}$ mice, consistent with a reduction in food intake ($P < 0.1$; $n = 8$; **Fig. 3c**,**d**). Loss of *Magel2* expression therefore seems not to result in hyperphagic behavior in young mice but may contribute to the early postnatal feeding difficulties seen in PWS.

PWS is also associated with hypogonadism, resulting in reduced fertility. *Magel2*$^{m+/p-}$ mice of both sexes were able to breed. However, it was noted that the mating frequency of males declined by 16 weeks and eventually they ceased to mate. Female *Magel2*$^{m+/p-}$ mice

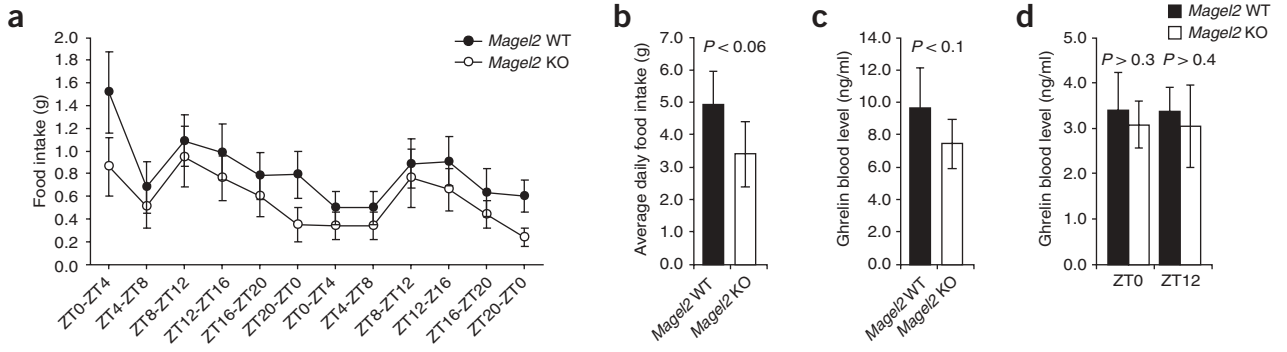

Figure 3 Breeding and feeding behavior is altered in *Magel2m+/p–* mice. (**a**) Food intake is reduced in *Magel2*$^{m+/p-}$ mice ($n = 8$) compared with *Magel2*$^{m+/p+}$ mice ($n = 7$) in 6- to 8-week-old animals. Mice were starved for 24 h before having access to food *ad libitum* at ZT0. Food-consumption data points were recorded at 4-h intervals during two full circadian cycles and plotted as average intake (in grams) between ZT(x) and ZT($x + 4$). Filled circles correspond to *Magel2*$^{m+/p+}$ (WT) control cohort, whereas open circles represent *Magel2*$^{m+/p-}$ (KO) data. (**b**) Food consumption shown in **a**, integrated and represented as average daily food intake during a 24-h interval. (**c**) Systemic levels of ghrelin (in ng per ml of blood serum) are slightly but significantly lower in *Magel2*$^{m+/p-}$ KO ($n = 8$) than in *Magel2*$^{m+/p+}$ WT mice ($n = 7$) at ZT0, immediately after the 24-h starvation. (**d**) The same cohort of KO and WT control animals was allowed unrestricted access to food for >1 week, and ghrelin was quantified from blood samples collected at ZT0 and ZT12, corresponding to the start of the light and dark phases, respectively. These results revealed no substantial difference in ghrelin levels.

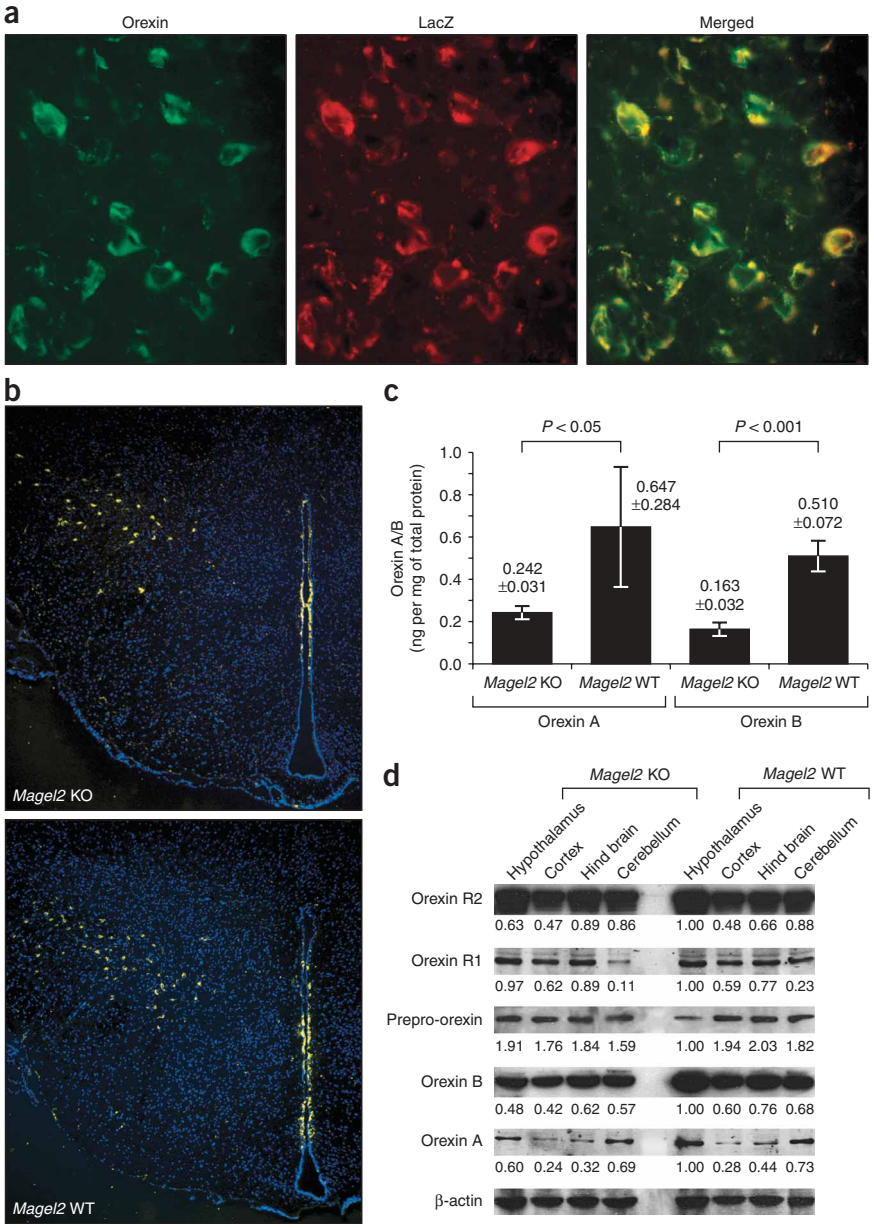

Figure 4 Orexin expression is reduced in *Magel2*-deficient animals. (**a**) Orexin B is coexpressed with Magel2 in neurons in the LVH. Left, orexin B staining of cells. Middle, LacZ staining of Magel2. Right, merged images. (**b**) Distribution of orexin B–immunoreactive neurons in the lateral hypothalamus of *Magel2*$^{m+/p-}$ (KO) and control wild-type (WT) mice. Coronal sections were collected at the level of the hypothalamic arcuate nucleus–median eminence, stained with orexin B–specific antibody, counterstained with DAPI and scored. Numbers of orexin-positive neurons (yellow staining) are reduced in the *Magel2*$^{m+/p-}$ mice (upper image). (**c**) Enzyme-linked immunoassay was used to quantify the amounts of orexin A and orexin B neuropeptides in the LVH. Both peptides are significantly less abundant in the *Magel2*$^{m+/p-}$ mice at the time of maximal *Magel2* expression during the subjective day. (**d**) Western blotting analysis of orexin signaling components. Equal amounts of total protein isolated from the indicated brain regions were probed with antibodies specific for orexin neuropeptides as well as for both of the orexin receptors. Only the hypothalamic samples from the *Magel2*$^{m+/p-}$ mice had detectably lower signal intensities of the orexin A and B peptides, consistent with the immunoassay results. In contrast, prepro-orexin levels in the hypothalamus were almost twofold higher in KO mice. Expression of orexins in all other regions of the brain was equivalent between the two groups. Orexin receptor levels were also largely unaffected, except that orexin receptor-2 levels were about 50% lower in the hypothalamus of the *Magel2*$^{m+/p-}$ mice and orexin receptor-1 levels were reduced some 50% in the cerebellum of the mutant mice. A β-actin–specific antibody was used as a loading control. The band intensities were quantified relative to the amount of actin, used as a loading control, with NIH Image.

remained fertile and produced multiple litters throughout their lifespans (**Supplementary Table 2** online). Testis weights and spermatogenesis seemed to be normal (**Supplementary Fig. 3** online), and the basis of the decline in male fertility remains unclear.

As *Magel2*$^{m+/p-}$ mice showed altered breeding and feeding behavior, as well as altered patterns of wakefulness, we analyzed the expression of four hypothalamic neuropeptides implicated in regulating these behaviors: the orexins (hypocretins), vasopressin, VIP and oxytocin[18,19]. In the lateral hypothalamus, orexins are coexpressed in neurons expressing *Magel2* (**Fig. 4a**). Orexin-expressing neurons are noteworthy in that they project throughout the brain, particularly in regions implicated in regulation of sleep, wakefulness, feeding and body temperature[20]. However, at the time of peak *Magel2* expression, the amounts of orexin A and B peptide in the dorsomedial region of the hypothalamus were about 60% lower in the *Magel2*$^{m+/p-}$ mice than in wild-type mice (**Fig. 4b,c**). This decrease correlated with a 40% reduction in orexin-positive neurons in the lateral hypothalamus (mean numbers of orexin-positive neurons: *Magel2*$^{m+/p+}$, 53 ± 11; *Magel2*$^{m+/p-}$, 33 ± 9; $P < 0.01$; **Fig. 4b,c** and **Supplementary Table 3** online). A western analysis of different regions of the brain receiving synaptic inputs from orexin-positive neurons indicated that orexin levels were primarily reduced in the hypothalamus and not in other regions of the CNS. Paradoxically, prepro-orexin levels were increased in the *Magel2*$^{m+/p-}$ hypothalamus by almost twofold (**Supplementary Table 3**). The basis of this discrepancy is not clear, although preliminary evidence (C.L.S. and S.V.K., unpublished observations) indicates that Magel2 maybe involved in post-translational processing, suggesting that the reduction in orexin levels is a consequence of inefficient processing of prepro-orexin. Consistent with a post-translational role of Magel2 in regulating orexin levels, the abundance of prepro-orexin mRNA was similar in both wild-type and *Magel2*$^{m+/p-}$ mice (**Supplementary Table 3**). The abundance of orexin-1 receptors in most regions of the CNS was largely unaffected by the loss of *Magel2* expression, with the possible exception of the cerebellum (**Fig. 4d**). In contrast, the amount of orexin-2 receptors seemed to be substantially reduced in the hypothalamus (**Fig. 4d**), possibly owing to orexin and ORX2 receptor levels being coregulated by some feedback mechanism[21]. Quantification of the other

hypothalamic-SCN neuropeptides at the time of peak *Magel2* expression, including oxytocin, VIP and vasopressin (which shows marked diurnal variation in expression), revealed no substantial differences in expression between wild-type and *Magel2*$^{m+/p-}$ mice ($n = 6$; data not shown).

The role of genomic imprinting in regulating CNS development and establishing postnatal behavior is a persisting puzzle[22]. The major hypothesis as to the function of genomic imprinting in mammals has centered on allocation of resources from the mother to the developing pre- and postnatal embryo. Paternally expressed imprinted genes favor the increased allocation of resources to the embryo, thus enhancing the survival of the father's genome in his offspring, to the detriment of the mother. To counteract this increased allocation, maternally expressed imprinted genes restrict the allocation of resources to the embryo. As the hypothalamus regulates feeding, energy metabolism and reproduction, any disruption of these activities would be potentially detrimental to the offspring's fitness. Previous studies have suggested that paternally expressed imprinted genes are important for hypothalamic development[23] and that specific paternally expressed genes, such as *Peg3* and *Mest*, are important for the proper maternal care of newborn offspring[24,25]. Our results now show that among the paternally expressed genes, *Magel2* is required for proper hypothalamic function in regulating circadian output, food intake and fertility in males, functions that maybe mediated by Magel2 via the regulation of orexin levels and/or the development of orexin-expressing neurons.

METHODS

Targeting the *Magel2* locus. Gene targeting of the *Magel2* locus was done according to standard procedures in Bruce4 C57Bl6 embryonic stem cells[26]. The targeting strategy and genotyping are shown in **Supplementary Figure 1a,b**. All procedures were approved by the Animal Care and Use Committee of the US National Institutes of Health (NIH) and conformed to NIH guidelines. Bacterial artificial chromosome (BAC) clone RPCI24-232N8 was used to construct a targeting vector to eliminate the open reading frame of *Magel2* gene and replace it with an in-frame LacZ expression cassette that would mark cells expressing Magel2 protein *in vivo*. To confirm correct targeting of *Magel2*, an *Eco*RI restriction length fragment polymorphism was used to detect the *Magel2* wild-type and null alleles (**Supplementary Fig. 1b**). One correctly targeted clone, number 22, was then used to establish a colony of *Magel2*-deficient mice using standard techniques that were maintained on a C57Bl/6 genetic background. Genotyping and RT-PCR primers are listed in **Supplementary Table 4** online.

Locomotor analysis. Mice were maintained in 12 h/12 h light/dark schedule (lights on at 7 a.m.) in the Hilltop animal facility at Washington University. Wild-type ($n = 8$ males and 3 females) and *Magel2*$^{m+/p-}$ mice ($n = 5$ males and 4 females) were housed individually with a running wheel, beginning at an age of approximately 8 months. Wheel revolutions per minute were recorded and the daily onsets of activity, free-running period, average daily activity and amplitude of rhythmicity were calculated using Clocklab software (Actimetrics) as previously described[27].

***In situ* hybridization.** *In situ* hybridization of *Magel2* mRNA was performed with mice killed in a light-dark schedule at 4-h intervals ($n = 3$ per time point, 18 females) or in constant darkness at four times relative to the animals' locomotor activity onset ($n = 3$ per time point, 5 males and 7 females). The time of light onset was defined as Zeitgeber time 0 (ZT0), and the time of light offset was ZT12. Circadian time 12 (CT12) was defined as the beginning of subjective night by the onset of locomotor activity. Animals whose brains were collected at time points in the dark were enucleated in the dark under infrared illumination immediately before perfusion. The mice were anesthetized with 1.5% Avertin and perfused directly into the left ventricle with 30 ml PBS followed by 35 ml of 4% paraformaldehyde and 4% sucrose in PBS. The brains were submerged in 4% paraformaldehyde and 4% sucrose for 24 h at 4 °C, cryoprotected in 10% sucrose for an additional 24 h at 4 °C, flash-frozen in Tissue-Tek O.C.T. Compound (Sakura Finetek USA) and kept at –80 °C until sectioning. Coronal, 20-µm sections of the brain were cut on a cryostat and collected onto sets of six slides, so that each slide contained a rostral-caudal series taken at 120-µm intervals.

The ^{33}P-labeled RNA probes were transcribed from a DNA template (GenBank AA049350) targeted at bases 1059–1679 of the *Magel2* mRNA (GenBank NM_013779) using a Riboprobe *in vitro* transcription kit (Promega). All *in situ* assays were performed according to a protocol adapted from ref. 28. Sections were hybridized with the radioactive *Magel2* RNA probe overnight at either 63 °C (light-dark brains) or 65 °C (constant-darkness brains), washed at 68 °C and then exposed on film overnight, for a total of three brains per time point.

Films were developed and then scanned at a resolution of 1,200 dots per inch, and the digital images were analyzed using Scion Image version 4.0.2 (Scion Corporation). *Magel2* expression in identified brain structures[29] was measured as the average OD within the area of the structure after subtraction of the background signal in a neighboring brain region of the same area.

LacZ histochemistry and immunohistochemistry. Paternal heterozygous and wild-type control littermate mice were perfused intracardiacally with 4% paraformaldehyde, and brains were removed, post-fixed and cryoprotected in 25% sucrose overnight. Eight-micron-thick sections were collected in either the coronal or horizontal plane and either incubated with primary antibodies to bacterial β-galactosidase (mouse monoclonal, Promega, diluted 1:200), VIP (rabbit polyclonal, ImmunoStar, diluted 1:300) and arginine-vasopressin peptide (rabbit polyclonal, ImmunoStar, diluted 1:500), and stained with DAPI (Molecular Probes). Some sections were processed to visualize the LacZ activity according to standard protocols. Embryos were collected from either timed-pregnant wild-type females mated with heterozygous *Magel2* males or from reciprocal crosses, fixed in 1% formalin and 0.25% glutaraldehyde, stained for LacZ activity, dehydrated in ethanol and cleared in benzyl benzoate solution.

Orexin neuropeptide and orexin receptor protein extracts for quantification were prepared from various brain regions of *Magel2*$^{m+/p-}$ mice and control wild-type littermates. Twenty micrograms of total protein were analyzed by ECL western blotting using the following antibodies obtained from Chemicon: anti–prepro-orexin (AB3096, diluted 1:100), anti–orexin A (AB3098, diluted 1:500), anti–orexin B (AB3100, diluted 1:500), anti–orexin-1 receptor (AB3092, diluted 1:200) and anti–orexin-2 receptor (AB3094, diluted 1:200).

To quantify lateral hypothalamic neurons expressing orexins, serial cryosections were cut coronally at 8-µm intervals to include brain regions with Bregma –1.10/–1.90. Sections were stained with orexin B–specific goat polyclonal antiserum (Santa Cruz, diluted 1:50) and positive neurons were scored on six to eight sections containing the maximum amount of positive cells. For enzyme-linked immunoassay analyses, brain tissue samples were collected to include lateral hypothalamic areas and sonicated for 30 s in 0.025 N HCl. Upon protein extraction during 1 h incubation on ice, samples were neutralized with NaOH and subjected to enzyme immunoassays (orexin B enzyme-linked immunoassay kit, Peninsula Laboratories) according to the manufacturer's recommendations.

Note: Supplementary information is available on the Nature Genetics website.

ACKNOWLEDGMENTS

This work was supported by the Intramural Research Program of the National Cancer Institute, NIH grants MH63104 (EDH) and EY14988, and the Culpeper Medical Scientist Award of the Rockefeller Brothers Foundation (to R.N.V.G.). We thank R. Seeley for advice, R. Awashti for help in the fertility assays, and R. Frederickson for help in preparation of the figures.

AUTHOR CONTRIBUTIONS

R.N.V.G., S.V.K., E.D.H., R.W., J.B.H., L.J.M. and C.L.S. designed the experiments, S.V.K., S.P., M.P.H. and J.W.B. performed the experiments, and R.V.G., E.D.H. and C.L.S. wrote the paper.

Published online at http://www.nature.com/naturegenetics
Reprints and permissions information is available online at http://npg.nature.com/reprintsandpermissions

1. Goldstone, A.P. Prader-Willi syndrome: advances in genetics, pathophysiology and treatment. *Trends Endocrinol. Metab.* **15**, 12–20 (2004).

2. Runte, M. *et al.* The IC-SNURF-SNRPN transcript serves as a host for multiple small nucleolar RNA species and as an antisense RNA for UBE3A. *Hum. Mol. Genet.* **10**, 2687–2700 (2001).
3. Bressler, J. *et al.* The SNRPN promoter is not required for genomic imprinting of the Prader-Willi/Angelman domain in mice. *Nat. Genet.* **28**, 232–240 (2001).
4. Yang, T. *et al.* A mouse model for Prader-Willi syndrome imprinting-centre mutations. *Nat. Genet.* **19**, 25–31 (1998).
5. Gerard, M., Hernandez, L., Wevrick, R. & Stewart, C.L. Disruption of the mouse *necdin* gene results in early post-natal lethality. *Nat. Genet.* **23**, 199–202 (1999).
6. Pagliardini, S., Ren, J., Wevrick, R. & Greer, J.J. Developmental abnormalities of neuronal structure and function in prenatal mice lacking the prader-willi syndrome gene necdin. *Am. J. Pathol.* **167**, 175–191 (2005).
7. Tsai, T.F., Jiang, Y.H., Bressler, J., Armstrong, D. & Beaudet, A.L. Paternal deletion from Snrpn to Ube3a in the mouse causes hypotonia, growth retardation and partial lethality and provides evidence for a gene contributing to Prader-Willi syndrome. *Hum. Mol. Genet.* **8**, 1357–1364 (1999).
8. Muscatelli, F. *et al.* Disruption of the mouse Necdin gene results in hypothalamic and behavioral alterations reminiscent of the human Prader-Willi syndrome. *Hum. Mol. Genet.* **9**, 3101–3110 (2000).
9. Ren, J. *et al.* Absence of Ndn, encoding the Prader-Willi syndrome-deleted gene necdin, results in congenital deficiency of central respiratory drive in neonatal mice. *J. Neurosci.* **23**, 1569–1573 (2003).
10. Boccaccio, I. *et al.* The human MAGEL2 gene and its mouse homologue are paternally expressed and mapped to the Prader-Willi region. *Hum. Mol. Genet.* **8**, 2497–2505 (1999).
11. Lee, S. *et al.* Expression and imprinting of MAGEL2 suggest a role in Prader-willi syndrome and the homologous murine imprinting phenotype. *Hum. Mol. Genet.* **9**, 1813–1819 (2000).
12. Lee, S., Walker, C.L. & Wevrick, R. Prader-Willi syndrome transcripts are expressed in phenotypically significant regions of the developing mouse brain. *Gene Expr. Patterns* **3**, 599–609 (2003).
13. Panda, S. *et al.* Coordinated transcription of key pathways in the mouse by the circadian clock. *Cell* **109**, 307–320 (2002).
14. Card, J.P. Pseudorabies virus and the functional architecture of the circadian timing system. *J. Biol. Rhythms* **15**, 453–461 (2000).
15. Ibata, Y. *et al.* Functional morphology of the suprachiasmatic nucleus. *Front. Neuroendocrinol.* **20**, 241–268 (1999).
16. Silver, R. & Schwartz, W.J. The suprachiasmatic nucleus is a functionally heterogeneous timekeeping organ. *Methods Enzymol.* **393**, 451–465 (2005).
17. Yoo, S.H. *et al.* PERIOD2:LUCIFERASE real-time reporting of circadian dynamics reveals persistent circadian oscillations in mouse peripheral tissues. *Proc. Natl. Acad. Sci. USA* **101**, 5339–5346 (2004).
18. Goldstone, A.P. The hypothalamus, hormones, and hunger: alterations in human obesity and illness. *Prog. Brain Res.* **153**, 57–73 (2006).
19. Sakurai, T. Roles of orexin/hypocretin in regulation of sleep/wakefulness and energy homeostasis. *Sleep Med. Rev.* **9**, 231–241 (2005).
20. Hara, J., Yanagisawa, M. & Sakurai, T. Difference in obesity phenotype between orexin-knockout mice and orexin neuron-deficient mice with same genetic background and environmental conditions. *Neurosci. Lett.* **380**, 239–242 (2005).
21. Willie, J.T. *et al.* Distinct narcolepsy syndromes in Orexin receptor-2 and Orexin null mice: molecular genetic dissection of Non-REM and REM sleep regulatory processes. *Neuron* **38**, 715–730 (2003).
22. Davies, W., Isles, A.R. & Wilkinson, L.S. Imprinted gene expression in the brain. *Neurosci. Biobehav. Rev.* **29**, 421–430 (2005).
23. Keverne, E.B., Fundele, R., Narasimha, M., Barton, S.C. & Surani, M.A. Genomic imprinting and the differential roles of parental genomes in brain development. *Brain Res. Dev. Brain Res.* **92**, 91–100 (1996).
24. Lefebvre, L. *et al.* Abnormal maternal behaviour and growth retardation associated with loss of the imprinted gene *Mest*. *Nat. Genet.* **20**, 163–169 (1998).
25. Li, L. *et al.* Regulation of maternal behavior and offspring growth by paternally expressed Peg3. *Science* **284**, 330–333 (1999).
26. Kontgen, F., Suss, G., Stewart, C., Steinmetz, M. & Bluethmann, H. Targeted disruption of the MHC class II Aa gene in C57BL/6 mice. *Int. Immunol.* **5**, 957–964 (1993).
27. Herzog, E.D., Aton, S.J., Numano, R., Sakaki, Y. & Tei, H. Temporal precision in the mammalian circadian system: a reliable clock from less reliable neurons. *J. Biol. Rhythms* **19**, 35–46 (2004).
28. Simmons, D.M., Arriza, J.L. & Swanson, L.W. A complete protocol for *in situ* hybridization of messenger RNAs in brain and other tissue with radio-labeled single stranded RNA probe. *J. Histotechnol.* **12**, 169–180 (1989).
29. Paxinos, G. & Tork, I. Neuroanatomical nomenclature. *Trends Neurosci.* **13**, 169 (1990).